HHS Public Access

Author manuscript

Eur Urol. Author manuscript; available in PMC 2024 September 01.

Published in final edited form as:

Eur Urol. 2023 September ; 84(3): 275–286. doi:10.1016/j.eururo.2023.02.016.

Phase 2 Trial of Stereotactic Ablative Radiotherapy for Patients with Primary Renal Cancer

Raquibul Hannan[a,b,*], **Mark F. McLaughlin**[a], **Laurentiu M. Pop**[a], **Ivan Pedrosa**[b,c,d], **Payal Kapur**[b,d,e], **Aurelie Garant**[a,b], **Chul Ahn**[b,f], **Alana Christie**[b], **James Zhu**[g], **Tao Wang**[g], **Liliana Robles**[a], **Deniz Durakoglugil**[a], **Solomon Woldu**[b,d], **Vitaly Margulis**[b,d], **Jeffrey Gahan**[b,d], **James Brugarolas**[b,h], **Robert Timmerman**[a,b], **Jeffrey Cadeddu**[b,d]

[a]Department of Radiation Oncology, University of Texas Southwestern, Dallas, TX, USA

[b]Kidney Cancer Program, Simmons Comprehensive Cancer Center, University of Texas Southwestern Medical Center, Dallas, TX, USA

[c]Department of Radiology, University of Texas Southwestern, Dallas, TX, USA

[d]Department of Urology, University of Texas Southwestern, Dallas, TX, USA

[e]Department of Pathology, University of Texas Southwestern, Dallas, TX, USA

[f]Department of Population and Data Sciences, University of Texas Southwestern, Dallas, TX, USA

[g]Quantitative Biomedical Research Center, Department of Population and Data Sciences, University of Texas Southwestern Medical Center, Dallas, TX, USA

[h]Department of Internal Medicine, University of Texas Southwestern, Dallas, TX, USA

Abstract

Background: Most renal cell carcinomas (RCCs) are localized and managed by active surveillance, surgery, or minimally invasive techniques.

[*]Corresponding author. Departments of Radiation Oncology and Immunology, University of Texas Southwestern Medical Center, 2280 Inwood Road, Dallas, TX 75390-9303, USA. Tel. +1 214-645-7696; Fax: +1 216-645-7624., Raquibul.Hannan@utsouthwestern.edu (R. Hannan).

***Author contributions*:** Raquibul Hannan had full access to all the data in the study and takes responsibility for the integrity of the data and the accuracy of the data analysis.

Study concept and design: Hannan, Timmerman, Brugarolas, Cadeddu.

Acquisition of data: Hannan, McLaughlin, Christie, Robles, Durakoglugil, Pop, Pedrosa, Kapur.

Analysis and interpretation of data: Hannan, Christie, McLaughlin, Ahn, Zhu.

Drafting of the manuscript: Hannan, McLaughlin.

Critical revision of the manuscript for important intellectual content: Hannan, Brugarolas, Timmerman, Pop, Pedrosa, Kapur, Garant, Ahn, Christie, Zhu, Wang, Robles, Durakoglugil, Woldu, Margulis, Gahan, Brugarolas, Timmerman, McLaughlin, Cadeddu.

Statistical analysis: Christie, Ahn.

Obtaining funding: Hannan.

Administrative, technical, or material support: Timmerman.

Supervision: Hannan, Brugarolas, Timmerman.

Other: Patient screening and enrollment: Hannan, Garant, Margulis, Gahan, Timmerman, Cadeddu, Woldu, Gahan.

Objective: To investigate whether stereotactic ablative radiotherapy (SAbR) may provide an innovative noninvasive alternative, although prospective data are limited.

Design, setting, and participants: Patients with biopsy-confirmed radiographically enlarging primary RCC (≤5 cm) were enrolled. SAbR was delivered in either three (12 Gy) or five (8 Gy) fractions.

Outcome measurements and statistical analysis: The primary endpoint was local control (LC) defined as a reduction in tumor growth rate (compared with a benchmark of 4 mm/yr on active surveillance) and pathologic evidence of tumor response at 1 yr. Secondary endpoints included LC by the Response Evaluation Criteria in Solid Tumors (RECIST 1.1), safety, and preservation of kidney function. Pre- and post-treatment biopsy samples were collected for exploratory tumor cell−enriched spatial protein and gene expression studies.

Results and limitations: Sixteen ethnically diverse patients were enrolled. Radiographic LC at 1 yr was observed in 94% (15/16; 95% confidence interval: 70, 100) of patients, and this was accompanied by pathologic evidence of tumor response (hyalinization, necrosis, and reduced tumor cellularity). By RECIST, 100% of the sites remained without progression at 1 yr. The median pretreatment growth rate was 0.8 cm/yr (interquartile range [IQR]: 0.3, 1.4), and the median post-treatment growth rate was 0.0 cm/yr (IQR: −0.4, 0.1, $p < 0.002$). Tumor cell viability decreased from 4.6% to 0.7% at 1 yr ($p = 0.004$). With a median follow-up of 36 mo for censored patients, the disease remained controlled in 94% of patients. SAbR was well tolerated with no grade ≥2 (acute or late) toxicities. The average glomerular filtration rate declined from a baseline of 65.6 to 55.4 ml/min at 1 yr ($p = 0.003$). Spatial protein and gene expression analyses were consistent with the induction of cellular senescence by radiation.

Conclusions: The evidence supports that SAbR safely controls ≤5 cm primary RCC, warranting further investigation in phase 3 trials.

Patient summary: In this clinical trial, we investigated a novel noninvasive treatment option of stereotactic radiation therapy for the treatment of primary kidney cancer. We found that stereotactic radiation was safe and effective for the treatment of primary kidney cancers.

Keywords

Primary renal cell carcinoma; Renal cell carcinoma; Stereotactic ablative radiotherapy; Senescence

1. Introduction

Kidney cancer (renal cell carcinoma [RCC]) is one of the ten most common malignancies for both incidence and mortality, with estimated 79 000 new cases in 2022 [1]. The incidental detection of small, localized kidney cancers has increased with the use of imaging [2,3]. Presently, 65% of patients with kidney cancer have localized disease and carry a 5-yr relative survival rate of 93% [4]. The standard of care for curative-intent local treatment is partial or radical nephrectomy, which is associated with perioperative mortality rates of ~1.4% in contemporary series [5]. Ablative techniques such as radiofrequency ablation (RFA) and cryoablation have shown promising outcomes. However, the location of some tumors precludes their application, and these are invasive, although minimally [6]. RCC

has been regarded as a “radioresistant” tumor, which is supported by in vitro studies [7], but high rates of local control (LC) have been achieved with high doses per fraction using stereotactic radiosurgery or stereotactic ablative radiotherapy (SAbR) [8–11].

Rapid and innovative advances in image guidance, respiratory motion assessment, and motion management techniques have enabled highly conformal and ablative radiation dose delivery to areas of the body that were technologically difficult, such as the kidneys. In particular, SAbR for primary RCC showed promising LC rates, despite limited prospective data [9,12–19]. However, most studies focused on radiographic LC, and there are limited prospective data showing reduced tumor viability [17,20]. This is particularly important as tumor enhancement is typically unchanged after radiation, even when tumors regress [21]. This is in contrast with RFA or cryoablation, where radiographic enhancement is typically reduced [22]. One possible explanation for these differences is the variable impact of the different treatment modalities on tumor vasculature.

In this prospective phase 2 trial of patients with biopsy-proven, radiographically progressive primary RCC treated with SAbR, we investigated the impact of SAbR on tumor growth radiographically as well as through pathologic studies. In addition, we performed spatially enriched analyses of protein and RNA expression of residual cancer cells to derive insights on the effects of radiation on senescence pathways.

2. Patients and methods

This prospective clinical trial was approved by the institutional review board at the University of Texas Southwestern Medical Center (STU 122013–030) and registered with clinicaltrials.gov (NCT02141919). After providing informed consent, 16 patients were enrolled between September 2014 and October 2019. All adult patients had biopsy-proven, localized, primary RCC that measured ≤5 cm with established radiographic growth (confirmed with a contrast-enhanced computed tomography [CT] scan or magnetic resonance imaging [MRI]) during the previous year. The exclusion criteria included previous treatment to the primary tumor, abdominal radiation, evidence of metastatic disease, and pregnancy. All patients were evaluated by a multidisciplinary team and offered trial enrollment as an option regardless of surgical resectability. The primary endpoint was LC, as defined by an increase in the longest tumor diameter of <4 mm from baseline and pathologic evidence of tumor response. The radiographic endpoint of <4 mm growth was adapted from previous reports of an average growth of 4 mm/yr in biopsy-proven RCC under active surveillance [23]. The secondary endpoints included LC by the Response Evaluation Criteria in Solid Tumors (RECIST) version 1.1, tumor growth rate, adverse events, locoregional and systemic progression, kidney function (as assessed by creatinine and renal perfusion mercaptoacetyltriglycine lasix renal scan at baseline and at 1 yr), and pathologic response correlates (as determined by pre- and post-treatment biopsies). All endpoints required a minimum follow-up of 12 mo.

Pretreatment assessment included complete history and physical examination, urinalysis, serum chemistries, blood counts, pregnancy testing (if applicable), nuclear medicine renal scan, biopsy of the renal mass, and serial cross-sectional imaging (ie, CT or MRI).

Radiation planning and delivery details have been described previously [24]. Briefly, radiation planning CT simulation was performed with vac-lok bag (Bionix SecureVac), stereotactic body frame (Elekta), four-dimensional CT assessment, and motion management. Intravenous contrast and MRI image registration were used when possible. Patients were treated with conventional c-arm linear accelerators (Varian Truebeam or Vitalbeam, Elekta Versa) using daily image guidance. Radiation doses were either 36 or 40 Gy delivered in three or five fractions, respectively. Trial dose levels were chosen based on equivalence using the universal survival model (173 vs 160 Gy) with an α/β ratio of 2.63, although a larger difference exists using the linear quadratic model (200 vs 162 Gy) [25]. Dose fractionation choice was primarily based on tumor location and proximity to the small bowel, at the discretion of the treating radiation oncologist relative to the ability to meet published protocol constraints [26]. Treatments were delivered a minimum of 40 h apart and were completed within 21 d. A characteristic treatment plan is illustrated in Figure 1.

Follow-up was performed 1 mo after treatment and every 6 mo thereafter for a period of up to 5 yr. The 1-mo follow-up involved complete history and physical examination, toxicity assessment, serum chemistries, blood counts, and urinalysis. Each subsequent 6-mo follow-up included the previous assessments and also contrast-enhanced MRI or CT to assess treatment response. Tumors were measured by a licensed radiologist specialized in genitourinary cancer and RCC. The estimated glomerular filtration rate (eGFR) was calculated using the chronic kidney disease epidemiology formula, which contains corrections for disparities based on sex and race. One year after treatment, nuclear medicine renal scanning and biopsy were repeated. Toxicity was assessed according to Common Terminology Criteria for Adverse Events (CTCAE) version 4.0. Immunohistochemistry (IHC) staining of both pre- and post-treatment tissue were performed following standard protocols in a Clinical Laboratory Improvement Amendments (CLIA)-certified laboratory and examined by a licensed pathologist specialized in genitourinary cancer and RCC who was blinded to the radiographic response.

An IHC analysis was performed on 3–5 μm formalin-fixed paraffin-embedded (FFPE) representative tissue sections using a Dako automated system (Agilent). A dual-staining protocol was used with carbonic anhydrase IX (1:400; red chromogen; Thermo Fischer) and Ki-67/MIB-1 (1:100, brown chromogen; Dako) to identify proliferating tumor cells in clear cell RCC tumors, and a single antibody (Ki-67/MIB-1) protocol was deployed for non−clear cell RCC. The IHC stains were evaluated with a 20× objective by an experienced genitourinary pathologist (P.K.) without knowledge of the clinicopathologic data. The number of tumor cells expressing Ki-67 over the total number of tumor cells present on the core biopsy was calculated. Results were represented as tumor cell percentages with nuclear Ki-67/MIB-1 staining for both pre- and post-treatment samples.

2.1. Spatial proteomic and transcriptomic analysis

Tumor cell−enriched spatial proteomic and whole transcriptomic profiling was performed using a NanoString GeoMx DSP platform (NanoString Technologies, Seattle, WA, USA) to detect protein and gene expression in FFPE primary tumor specimens from four patients (baseline and 1-yr post-treatment biopsies), as described previously [27]. Hematoxylin and

eosin (H&E) and the other markers (CAIX, CD31, CD45, and nuclear stain markers) were used to select the regions of interest (ROIs) comprising $CAIX^+$ $CD31^-$ $CD45^-$ tumor cells only (Supplementary Fig. 1). For proteomic investigation, the ROI was stained with a panel of antibodies targeting cell death, phosphoinositide 3-kinase (PI3K), and mitogen-activated protein kinase (MAPK) signaling pathways [27]. Next-generation sequencing (NGS) was performed on the enriched tumor cells in the ROI for whole transcriptomic sequencing in Illumina sequencers using GeoMx DSP NGS. A gene set enrichment analysis was performed to determine whether a set of genes showed statistically significant and/or concordant differences between two biological conditions [28].

2.2. Sample size calculation and statistical methods

According to previous retrospective and prospective studies, SAbR produces LC in approximately 90% of patients [13,16,17]. The LC rate and its 95% confidence interval (CI) were estimated using the exact binomial method. With a sample size of 16 patients, a single group *t* test with a two-sided 0.10 significance level will have 80% power to detect a reduction between a pretreatment tumor growth rate of 0.4 cm/yr and a post-treatment tumor growth rate of 0.16 cm/yr (a 60% reduction), assuming that the standard deviation of the change in growth rate from before to after treatment is 0.36 cm/yr.

Overall survival, progression-free survival, and time to progression were assessed using the Kaplan-Meier method. Changes in tumor growth rate, kidney split function, and eGFR between baseline and post-treatment period were tested using paired *t* tests. Hyalinization and Ki-67 values were analyzed before and after treatment using the Wilcoxon signed rank test. Presence or absence of necrosis before and after treatment was compared using the McNemar's test. A p value of <0.05 was considered significant.

A mixed-effect model analysis was used to look for significant differences in GeoMX DSP proteomic results between baseline and 1-yr post-treatment samples across all patients, with the samples from the same patient being modeled with a compound symmetric covariance structure. All tests were two tailed and analyzed at the 0.05 significance level with false discovery rate adjustment for multiple comparisons using SAS 9.4 (SAS Institute Inc., Cary, NC, USA).

3. Results

3.1. Patient characteristics and intervention

Sixteen of 20 screened patients were enrolled in the study between September 2014 and October 2019. Two patients were excluded due to their biopsies being outside the enrollment window. One patient was excluded because of an unsuccessful biopsy, and another for a synchronous diagnosis of lung cancer. Baseline patient characteristics are summarized in Table 1. There was a predominance of men and right-sided tumors, which reflects the incidence of RCC. Tumor T staging was predominantly T1a according to the American Joint Committee on Cancer eighth edition, with 3 T1b tumors. One patient had a congenital atrophic nontarget kidney (ie, contralateral), but all other patients had bilaterally functioning kidneys. RENAL (Radius, Exophytic/endophytic, Nearness to the collecting

system, Anterior/posterior, Location relative to the polar line) nephrometry scores were low (4−6, $n = 8$) or intermediate (7−9, $n = 8$; Table 1 and Supplementary Table 2) [29]. Neither the RENAL score nor surgical resectability was used as an eligibility criterion in the trial. All patients completed the prescribed radiation within the 3-wk time period allowed by the trial protocol. Most patients received 36 Gy in three fractions ($n = 10$, 63%), with the rest receiving 40 Gy in five fractions (Table 1 and Fig. 1).

3.2. Local control

All 16 patients had a decrease in their tumor growth rate at 1-yr after SAbR as compared with the growth rate prior to treatment (Fig. 2A and 2B). The mean change in tumor growth rate from before treatment to 1 yr after treatment was −1.3 cm/yr (95% CI: −2.0, −0.5; $p = 0.002$). The median pretreatment growth rate was 0.8 cm/yr (interquartile range [IQR]: 0.3, 1.4) and the median post-treatment growth rate was 0.0 cm/yr (IQR: −0.4, 0.1; Fig. 2B). Radiographic LC was achieved by 94% (15/16; 95% CI: 70, 100) of patients at 1 yr (Fig. 2A). Radiographic LC by RECIST was 100% at 1 yr, and LC by protocol criteria was 94% at 1 yr. Over the current observation period for the trial, 88% of patients (14/16) still demonstrate radiographic LC by protocol criteria and 94% (15/16) by RECIST at the last follow-up (Fig. 2B and Supplementary Fig. 2). The median follow-up was 36 mo for patients without an event. Partial response, defined as a decrease in the longest diameter by >30%, was seen in three patients (19%; Fig. 2B). Interestingly, as evident in Figure 2A, all three patients who achieved a partial response received three-fraction SAbR, although the sample size is not sufficient to determine the significance of the association between response and fractionation. They included patients with clear cell, chromophobe, and papillary subtypes. Ten patients (63%) had stable disease as per the protocol criteria and by RECIST. Representative radiologic imaging before and after treatment in a responding patient is shown in Figure 3.

Tumor tissue (both at baseline and 1 yr after treatment) was available for pathologic review in 12 out of 16 enrolled patients. A histologic analysis of the 1-yr post-treatment biopsy tissue revealed prominent hyalinization and fibrosis with reduced viable tumor cells. To assess the proliferative state of tumor cells, we performed IHC for Ki-67 (along with CAIX in ccRCC). We found a significant decrease ($p = 0.0078$) in Ki-67 positivity in the scant remaining tumor cells in post-treatment samples (median: 1%) as compared with pretreatment samples (median: 4%; Fig. 4). Post-treatment tissue, but not pretreatment biopsies, showed prominent hyalinization. Hyalinization is generally observed in tumors after treatment, with tumor regression [30,31]. We assessed the hyalinization amount in biopsies as a percentage of the total length of the core biopsy. A significant increase in hyalinization ($p = 0.0039$) was found from pretreatment (median: 0%) to post-treatment (median: 65%) period. In the 11 patients with tumor necrosis measured before and after treatment, the presence of necrosis was observed in four patients after treatment, only one of whom had necrosis before treatment, although this was not significant ($p = 0.08$). The key pathology data are summarized in Table 2. Dual CAIX/Ki-67 staining showed that Ki-67 was predominantly confined to tumor-infiltrating lymphocytes and endothelial cells (Fig. 4). Finally, p16, a marker for cellular senescence, was induced in tumor cells at 1 yr after radiation therapy (Fig. 4, bottom panel).

3.3. Adverse events

SAbR was well tolerated by trial participants. No grade ≥2 adverse events were observed that were deemed possibly, probably, or definitely related to radiation treatment. Overall, eight out of 16 patients experienced grade 1 acute toxicity (Table 3 and Supplementary Table 1). Nausea and vomiting were the most common side effects and accounted for about half of all adverse events, which were mostly acute and resolved at the time of the first follow-up in 6 wk. Only three adverse events developed or persisted after the initial 90-d period: increased creatinine in two patients, and thrombocytopenia and fatigue in one patient (Table 3 and Supplementary Table 1).

3.4. Impact on kidney function

After treatment, kidney function was assessed via eGFR and renal perfusion scanning; eGFR was available at baseline and after 1 yr for 15 patients, and was significantly decreased on average by 10.2 ml/min (95% CI: −16.3, −4.1; $p = 0.003$) from a median baseline of 61.2 to 56.7 ml/min. As an ad hoc analysis, we evaluated the baseline decline in the eGFR before SAbR in the 6−18 mo prior to trial enrollment. For the patients who had data available ($n = 5$), the baseline median annualized decline of eGFR was 7.6 ml/min (IQR: −7.9, −7.5). The same cohort of patients exhibited an eGFR decline of 12.8 ml/min (IQR: −18.4, 2.2) 1 yr after treatment, which was not statistically different from their baseline decline ($p = 0.6$). Longer-term follow-up shows a nonsignificant decline in mean eGFR at 24 mo compared with that at baseline (−4.0 ml/min; 95% CI: −8.1, 0.1; $p = 0.053$; $n = 10$). The differences in mean eGFR were again significant at 36 mo (−12.1 ml/min; 95% CI: −19.6, −4.6; $p = 0.0065$; $n = 8$) and at the longest follow-up for each patient (median follow-up 35.4 mo; −10.3 ml/min; 95% CI: −18.3, −2.2; $p = 0.016$; $n = 16$). No significant differences ($p > 0.10$) were detected in eGFR decline at 12 mo based on race/ethnicity.

Kidney split function from renal perfusion scan was available at baseline and at 1 yr for 13 patients. Target kidney filtration represented a median of 47% of total kidney function at baseline. Split function showed a statistically significant decrease after SAbR to 40% (mean change: 6.4; 95% CI: 3.8, 9.0; $p = 0.0001$).

3.5. Local failure

Two patients (108 and 115; Table 2) developed radiographic failure (≥4 mm growth per year) by protocol criteria, with one of them also exhibiting radiographic failure by RECIST criteria (patient 108). One of the patients had papillary RCC (grade 2 on biopsy) and received 36 Gy in three fractions (Fig. 2D). A pathologic analysis before and after SAbR showed a decrease in Ki-67 from 15% to 1% and an increase in hyalinization. The second patient had clear cell RCC (grade 3 on biopsy) and received 40 Gy in five fractions. The patient initially presented with a 3.8-cm tumor, which grew to 4.3 cm at 30 mo (Fig. 2D). A pathologic analysis showed an initial Ki-67 of 10%, which decreased to 1% at 1 yr. The patient continues to be observed. Unfortunately, no tissue was available at the time of failure for comparison purposes from either patient.

To date, no patients developed regional or distant metastases. During the follow-up period, five patients died of unrelated causes (four patients from cardiovascular disease and one

from end-stage liver disease) at 2.1, 2.3, 2.8, 3.0, and 4.7 yr after treatment, indicating 3-yr overall survival of 79% (95% CI: 47, 93) and cancer-specific mortality of 0% (Fig. 2C).

3.6. Tumor cell protein and gene expression changes

Tumor cell−enriched spatial proteomic and whole transcriptomic profiling was performed on pre- and post-tumor biopsy tissue after ROI selection based on H&E and CAIX markers (Supplementary Fig. 1). When comparing tumor cells at 1 yr after radiation with those at baseline, there were no changes in cell death pathways, there was an increase in MAPK (six out of nine components, $p < 0.05$), and the levels of PI3K/AKT trended downward without reaching significance (Table 4). When the MAPK pathway was compared as a group with the rest, it was significantly upregulated (hypergeometric $p = 0.0004$). Gene set enrichment analyses of pre- and post-treatment samples enriched for tumor cells showed a reduction in apoptosis (Fig. 5A) and a biphasic response on cellular senescence (Fig. 5B).

4. Discussion

The present trial, one of the first phase 2 trials evaluating SAbR for primary RCC with endpoint analyses incorporating pathologic studies, met its predefined primary endpoint. The study showed LC rates of 94% (15/16) with pathologic evidence of response at 1 yr. All patients previously had growing tumors. Two patients eventually developed radiographic local failure (by a protocol analysis) despite histologic evidence of response at 1 yr, which highlights the need of additional biopsy sampling after SAbR and possibly the lack of an ideal histopathologic definition of local failure. Despite ultimate local failure, both tumors exhibited rapid growth prior to trial enrollment and showed decreased growth kinetics as a result of treatment (Fig. 2B). Treatment was well tolerated, and there were no grade ≥2 toxicities. However, a decline in renal function was observed.

The International Radiosurgery Oncology Consortium for Kidney (IROCK) reported 2-yr LC, cancer-specific survival, and progression-free survival of 98%, 96%, and 77% declining to 98%, 92%, and 65% at 4 yr, respectively [32]. Using comparable RECIST criteria, three patients had a partial response (19%) and one failure was observed (94%) with a median follow-up of 36 mo for patients censored in our study. Prior prospective clinical trials for primary RCC largely involved phase 1 studies on inoperable patients, lacked pathologic data, and typically had short follow-up periods [12,14–16,18,21]. In addition, half of these studies deployed robotic radiosurgery systems, which may not be feasible outside large academic centers [16,18,21]. An ongoing multicenter study, FASTRACK II, is evaluating SAbR safety and efficacy with a wide array of treatment platforms [33]. Dose escalation studies routinely showed no dose limiting toxicity [15,16,21]. One study reported intact tumor cells in H&E staining for five primary RCC patients after SAbR in an ad hoc analysis but did not investigate the reproductive potential of those cells [21]. A recent meta-analysis of 383 primary RCC cases treated with SAbR in 372 patients from 26 prospective and retrospective studies indicated a weighted random-effect estimate for LC of 97% at a median 28-mo follow-up, with most failures occurring with low-dose regimens [34]. A second IROCK study with an individual-level meta-analysis of 190 patients showed a local failure rate of 5.5% at 5 yr with reduced failure using single-fraction compared with multifraction

SAbR [35]. Consistent with this finding, and in-line with the pre-existing in vitro and in vivo literature supporting sensitivity of RCC to a larger dose per treatment, we also noticed a larger number of partial responses in our study in patients receiving three-fraction as compared with five-fraction SAbR, which did not reach statistical significance due to a small sample size (Fig. 2B) [7,36]. Overall, the high SAbR LC rate compares favorably with RFA and cryoablation (87% and 95%, respectively at a mean follow-up of 18.7 mo) [37].

Large primary tumors pose a particular challenge for minimally invasive management. At tumor sizes >3–4 cm, control rates decrease and complication rates increase with thermal techniques [38–40]. In our series, nine patients had baseline tumor sizes ≥3 cm, with three patients with tumors ≥4 cm including two with progressive disease. Nevertheless, the IROCK series showed a 4-yr local failure rate of 2.9% for primary kidney cancers ≥4 cm [41].

Unlike RAF or cryoablation, SAbR is not limited by tumor location within the kidney. Proximity to the renal pelvis is a contraindication to ablative techniques. In contrast, both exophytic and endophytic tumors, including those in proximity to the renal pelvis, are amenable to SAbR. Similarly, the RENAL nephrometry score also does not appear to impact treatability with SAbR. In the trial population, five patients had tumors ≤4 mm from the collecting system or renal sinus, three tumors were endophytic, while an additional three were entirely endophytic (Supplementary Table 2). Indeed, several patients enrolling in this trial were referred after they were deemed poor candidates for RAF or cryoablation due to tumor location. Furthermore, while it is conceivable that cases could exist where proximity to the small bowel precludes the delivery of adequately ablative radiation dose to an exophytic renal tumor that abuts a loop of small bowel, no patients were excluded from this study because of tumor location. This wide applicability represents a key advantage of SAbR over other ablative techniques.

SAbR was well tolerated. A random-effect estimate for grade 3/4 toxicity was 1.5% with no peritreatment mortality. These low toxicity rates occur in patients who have generally been deemed medically inoperable or have otherwise refused surgical treatment, likely reflecting a population with worse comorbidities than the general population.

Preserving kidney function remains the key for maintaining patient quality of life. None of the patients required dialysis after SAbR. SAbR was associated, however, with a 7.7 ml/min decline in eGFR [34], which is comparable with the reported 6.7 ml/min decline with RFA [42] or 10.0 ml/min decline with cryoablation [43]. Interestingly, while it is difficult to distinguish the effect of SAbR from the baseline decline, our analysis shows that an SAbR-induced decline in eGFR is a late effect of radiation that becomes significant at the 3-yr time of analysis, suggesting late fibrosis as a potential mechanism.

A revealing finding of this study is the identification of cellular senescence in rare surviving “viable” tumor cells 1 yr after SAbR. This is one of the first studies to demonstrate this late state of terminal replicative arrest induced by radiation in a prospective clinical trial. Tumor cells did not express Ki67, which likely results from damage to DNA and activation of the p53-p21-CDK2 and p16-CDK4-retinoblastoma (Rb) cell cycle checkpoint pathways

[44–46]. Our findings are consistent with the notion that SAbR induced cell death in the majority of the tumor cells (as demonstrated by the significant reduction in post-treatment cellularity). However, a minority of cells entered senescence, a state of irreversible cell cycle arrest as demonstrated by the changes in proteomics and transcriptomics, including the MAPK signaling pathway, well known for modulating cell survival, senescence-growth arrest, and senescence-associated secretory phenotype [47]. Although intact and perhaps metabolically active, these are “nonviable” tumor cells according to the classical definition of tumor cell viability, as defined by clonogenic cell survival assays that measures the ability of tumor cells to divide and form colonies in vitro or tumors in vivo [48]. In addition to the limitation of having a small sample size with limited tissue due to the post-SAbR tumor shrinkage, which was somewhat abrogated by having five to six ROIs per biopsy, a limitation of the 1-yr post-treatment biopsy analysis is that it provides a selection bias of the existing cells at 1-yr time point and precludes any inference on the chronology of events that led to that state, and hence additional cell death mechanism induced by SAbR at an earlier time point is likely under-represented.

Strengths of this study include its prospective phase 2 design, enrollment of biopsy-confirmed RCC tumors with pretreated growth, and a pathologic assessment after treatment. Limitations include the small size, and single-arm and single-institutional experience.

5. Conclusions

In summary, we report prospective data deploying a noninvasive technique, SAbR, for the control of primary RCC. Our study expands a growing body of literature that SAbR is able to control primary RCC with low toxicity rates, albeit with a reduction in renal function. Larger, prospective, randomized, multi-institutional studies with long-term follow-up are needed to fully establish the role of SAbR in treating primary kidney cancer.

Supplementary Material

Refer to Web version on PubMed Central for supplementary material.

Acknowledgments:

The authors acknowledge all the patients who participated in the study and their families. We credit Dr. Damiana Chiavolini for the scientific editing of the manuscript. The authors acknowledge the UTSW Kidney Cancer SPORE including the pathology core.

Funding/Support and role of the sponsor:

This clinical trial was funded by American Cancer Society (RSG-16-004-01-CCE; PI Raquibul Hannan). Raquibul Hannan is also funded by CPRIT RP180725 and P50CA196516. James Brugarolas, Payal Kapur, and Ivan Pedrosa are funded by P50CA196516. Payal Kapur and Ivan Pedrosa are funded by 5RO1CA154475. Ivan Pedrosa is funded by U01CA207091. Tao Wang is funded by NIH 5P30CA142543, NIH 1R01CA258584, and CPRIT RP190208.

Financial disclosures:

Raquibul Hannan certifies that all conflicts of interest, including specific financial interests and relationships and affiliations relevant to the subject matter or materials discussed in the manuscript (eg, employment/affiliation, grants or funding, consultancies, honoraria, stock ownership or options, expert testimony, royalties, or patents filed, received, or pending), are the following: None.

References

[1]. Siegel RL, Miller KD, Fuchs HE, Jemal A. Cancer statistics, 2022. CA Cancer J Clin 2022;72:7–33. [PubMed: 35020204]

[2]. Jayson M, Sanders H. Increased incidence of serendipitously discovered renal cell carcinoma. Urology 1998;51:203–5. [PubMed: 9495698]

[3]. Smith SJ, Bosniak MA, Megibow AJ, Hulnick DH, Horii SC, Raghavendra BN. Renal cell carcinoma: earlier discovery and increased detection. Radiology 1989;170(3 Pt 1):699–703. [PubMed: 2644658]

[4]. Howlader N, Noone AM, Krapcho M, et al., editors. SEER cancer statistics review, 1975−2017. Bethesda, MD: National Cancer Institute; April 2020. https://seer.cancer.gov/csr/1975_2017/

[5]. Fontenil A, Bigot P, Bernhard JC, et al. Who is dying after nephrectomy for cancer? Study of risk factors and causes of death after analyzing morbidity and mortality reviews (UroCCR-33 study). Progr Urol 2019;29:282–7.

[6]. Bianchi L, Mineo Bianchi F, Chessa F, et al. Percutaneous tumor ablation versus partial nephrectomy for small renal mass: the impact of histologic variant and tumor size. Minerva Urol Nefrol 2021;73:581–90.

[7]. Deschavanne PJ, Fertil B. A review of human cell radiosensitivity in vitro. Int J Radiat Oncol Biol Phys 1996;34:251–66. [PubMed: 12118559]

[8]. Corbin KS, Ranck MC, Hasselle MD, et al. Feasibility and toxicity of hypofractionated image guided radiation therapy for large volume limited metastatic disease. Pract Radiat Oncol 2013;3:316–22. [PubMed: 24674404]

[9]. Svedman C, Sandström P, Pisa P, et al. A prospective Phase II trial of using extracranial stereotactic radiotherapy in primary and metastatic renal cell carcinoma. Acta Oncol 2006;45:870–5. [PubMed: 16982552]

[10]. Zelefsky MJ, Greco C, Motzer R, et al. Tumor control outcomes after hypofractionated and single-dose stereotactic image-guided intensity-modulated radiotherapy for extracranial metastases from renal cell carcinoma. Int J Radiat Oncol Biol Phys 2012;82:1744–8. [PubMed: 21596489]

[11]. Balagamwala EH, Angelov L, Koyfman SA, et al. Single-fraction stereotactic body radiotherapy for spinal metastases from renal cell carcinoma. J Neurosurg Spine 2012;17:556–64. [PubMed: 23020208]

[12]. Siva S, Pham D, Kron T, et al. Stereotactic ablative body radiotherapy for inoperable primary kidney cancer: a prospective clinical trial. BJU Int 2017;120:623–30. [PubMed: 28188682]

[13]. Siva S, Pham D, Tan TH, et al. Principal analysis of a phase Ib trial of stereotactic body radiation therapy (SBRT) for primary kidney cancer. Int J Radiat Oncol Biol Phys 2016;96:S96.

[14]. Pham D, Thompson A, Kron T, et al. Stereotactic ablative body radiation therapy for primary kidney cancer: a 3-dimensional conformal technique associated with low rates of early toxicity. Int J Radiat Oncol Biol Phys 2014;90:1061–8. [PubMed: 25442039]

[15]. McBride SM, Wagner AA, Kaplan ID. A phase 1 dose-escalation study of robotic radiosurgery in inoperable primary renal cell carcinoma. Int J Radiat Oncol Biol Phys 2013;87:S84.

[16]. Kaplan ID, Redrosa I, Martin C, Collins C, Wagner A. Results of a phase I Dose escalation study of stereotactic radiosurgery for primary renal tumors. Int J Radiat Oncol Biol Phys 2010;78:S191.

[17]. Ponsky L, Lo SS, Zhang Y, et al. Phase I dose-escalation study of stereotactic body radiotherapy (SBRT) for poor surgical candidates with localized renal cell carcinoma. Radiother Oncol 2015;117:183–7. [PubMed: 26362723]

[18]. Staehler M, Bader M, Schlenker B, et al. Single fraction radiosurgery for the treatment of renal tumors. J Urol 2015;193:771–5. [PubMed: 25132240]

[19]. Siva S, Jackson P, Kron T, et al. Impact of stereotactic radiotherapy on kidney function in primary renal cell carcinoma: establishing a dose-response relationship. Radiother Oncol 2016;118:540–6. [PubMed: 26873790]

[20]. Grubb WR, Ponsky L, Lo SS, et al. Final results of a dose escalation protocol of stereotactic body radiotherapy for poor surgical candidates with localized renal cell carcinoma. Radiother Oncol 2020;155:138–43. [PubMed: 33214131]

[21]. Sun MR, Brook A, Powell MF, et al. Effect of stereotactic body radiotherapy on the growth kinetics and enhancement pattern of primary renal tumors. AJR Am J Roentgenol 2016;206:544–53. [PubMed: 26901010]

[22]. Kawamoto S, Permpongkosol S, Bluemke DA, Fishman EK, Solomon SB. Sequential changes after radiofrequency ablation and cryoablation of renal neoplasms: role of CT and MR imaging. Radiographics 2007;27:343–55. [PubMed: 17374857]

[23]. Chawla SN, Crispen PL, Hanlon AL, Greenberg RE, Chen DY, Uzzo RG. The natural history of observed enhancing renal masses: meta-analysis and review of the world literature. J Urol 2006;175:425–31. [PubMed: 16406965]

[24]. McLaughlin M, Kapur P, Pedrosa I, et al. A phase II trial of stereotactic ablative radiotherapy for patients with primary renal cell cancer. Int J Radiat Oncol Biol Phys 2020;108(3, Suppl):e865–6.

[25]. Park C, Papiez L, Zhang S, Story M, Timmerman RD. Universal survival curve and single fraction equivalent dose: useful tools in understanding potency of ablative radiotherapy. Int J Radiat Oncol Biol Phys 2008;70:847–52. [PubMed: 18262098]

[26]. Timmerman R A story of hypofractionation and the table on the wall. Int J Radiat Oncol Biol Phys 2022;112:4–21. [PubMed: 34919882]

[27]. Toki MI, Merritt CR, Wong PF, et al. High-plex predictive marker discovery for melanoma immunotherapy-treated patients using digital spatial profiling. Clin Cancer Res 2019;25:5503–12. [PubMed: 31189645]

[28]. Powers RK, Goodspeed A, Pielke-Lombardo H, Tan AC, Costello JC. GSEA-InContext: identifying novel and common patterns in expression experiments. Bioinformatics 2018;34:i555–64. [PubMed: 29950010]

[29]. Kutikov A, Uzzo RG. The R.E.N.A.L. nephrometry score: a comprehensive standardized system for quantitating renal tumor size, location and depth. J Urol 2009;182:844–53. [PubMed: 19616235]

[30]. Rao SR, Lazarides AL, Leckey BL, et al. Extent of tumor fibrosis/hyalinization and infarction following neoadjuvant radiation therapy is associated with improved survival in patients with soft-tissue sarcoma. Cancer Med 2022;11:194–206. [PubMed: 34837341]

[31]. Straub JM, New J, Hamilton CD, Lominska C, Shnayder Y, Thomas SM. Radiation-induced fibrosis: mechanisms and implications for therapy. J Cancer Res Clin Oncol 2015;141:1985–94. [PubMed: 25910988]

[32]. Siva S, Louie AV, Warner A, et al. Pooled analysis of stereotactic ablative radiotherapy for primary renal cell carcinoma: a report from the International Radiosurgery Oncology Consortium for Kidney (IROCK). Cancer 2018;124:934–42. [PubMed: 29266183]

[33]. Siva S, Chesson B, Bressel M, et al. TROG 15.03 phase II clinical trial of Focal Ablative STereotactic Radiosurgery for Cancers of the Kidney—FASTRACK II. BMC Cancer 2018;18:1030. [PubMed: 30352550]

[34]. Correa RJM, Louie AV, Zaorsky NG, et al. The emerging role of stereotactic ablative radiotherapy for primary renal cell carcinoma: a systematic review and meta-analysis. Eur Urol Focus 2019;5:958–69. [PubMed: 31248849]

[35]. Siva S, Ali M, Correa RJM, et al. 5-Year outcomes after stereotactic ablative body radiotherapy for primary renal cell carcinoma: an individual patient data meta-analysis from IROCK (the International Radiosurgery Consortium of the Kidney). Lancet Oncol 2022;23:1508–16. [PubMed: 36400098]

[36]. Walsh L, Stanfield JL, Cho LC, et al. Efficacy of ablative high-dose-per-fraction radiation for implanted human renal cell cancer in a nude mouse model. Eur Urol 2006;50:795–800; discussion 800. [PubMed: 16632182]

[37]. Kunkle DA, Uzzo RG. Cryoablation or radiofrequency ablation of the small renal mass: a meta-analysis. Cancer 2008;113:2671–80. [PubMed: 18816624]

[38]. Ramanathan R, Leveillee RJ. Ablative therapies for renal tumors. Ther Adv Urol 2010;2:51–68. [PubMed: 21789083]

[39]. Psutka SP, Feldman AS, McDougal WS, McGovern FJ, Mueller P, Gervais DA. Long-term oncologic outcomes after radiofrequency ablation for T1 renal cell carcinoma. Eur Urol 2013;63:486–92. [PubMed: 22959191]

[40]. Caputo PA, Zargar H, Ramirez D, et al. Cryoablation versus partial nephrectomy for clinical T1b renal tumors: a matched group comparative analysis. Eur Urol 2017;71:111–7. [PubMed: 27568064]

[41]. Siva S, Correa RJM, Warner A, et al. Stereotactic ablative radiotherapy for primary renal cell carcinoma: a report from the International Radiosurgery Oncology Consortium for Kidney (IROCK). Int J Radiat Oncol Biol Phys 2020;108:941–9. [PubMed: 32562838]

[42]. Raman JD, Thomas J, Lucas SM, et al. Radiofrequency ablation for T1a tumors in a solitary kidney: promising intermediate oncologic and renal function outcomes. Can J Urol 2008;15:3980–5. [PubMed: 18405445]

[43]. Staziaki PV, Vadvala HV, Furtado VF, Daye D, Arellano RS, Uppot RN. Early trends and predictors of renal function following computed tomography-guided percutaneous cryoablation of a renal mass in patients with and without prior renal impairment. Radiol Bras 2020;53:141–7. [PubMed: 32587420]

[44]. Gewirtz DA, Holt SE, Elmore LW. Accelerated senescence: an emerging role in tumor cell response to chemotherapy and radiation. Biochem Pharmacol 2008;76:947–57. [PubMed: 18657518]

[45]. Serrano M, Lin AW, McCurrach ME, Beach D, Lowe SW. Oncogenic ras provokes premature cell senescence associated with accumulation of p53 and p16INK4a. Cell 1997;88:593–602. [PubMed: 9054499]

[46]. Zhu J, Woods D, McMahon M, Bishop JM. Senescence of human fibroblasts induced by oncogenic Raf. Genes Dev 1998;12:2997–3007. [PubMed: 9765202]

[47]. Anerillas C, Abdelmohsen K, Gorospe M. Regulation of senescence traits by MAPKs. Geroscience 2020;42:397–408. [PubMed: 32300964]

[48]. Franken NA, Rodermond HM, Stap J, Haveman J, van Bree C. Clonogenic assay of cells in vitro. Nat Protoc 2006;1:2315–9. [PubMed: 17406473]

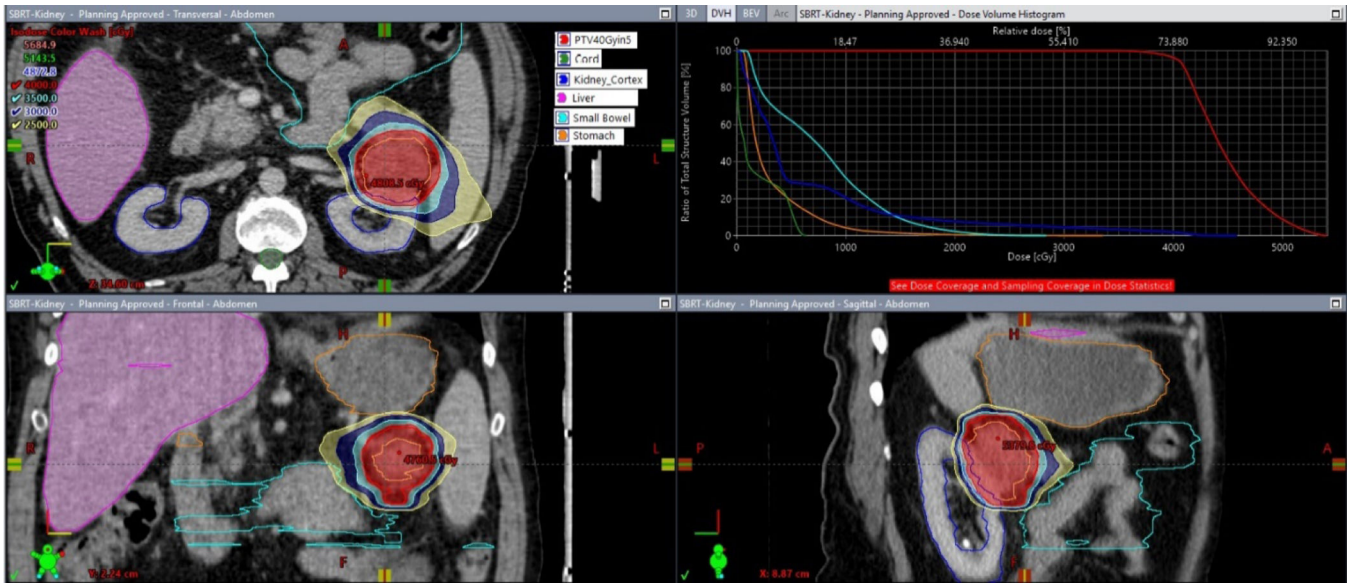

Fig. 1 –.

Representative patient treatment plan depicting axial (top left), coronal (bottom left), and sagittal (bottom right) views, along with a dose volume histogram. The 40 Gy in five fractions PTV is shown in red, kidney in blue, small bowel in cyan, stomach in orange, and liver in magenta. Dose color wash values are 40 Gy (red), 35 Gy (cyan), 30 Gy (blue), and 25 Gy (yellow). PTV = planning treatment volume.

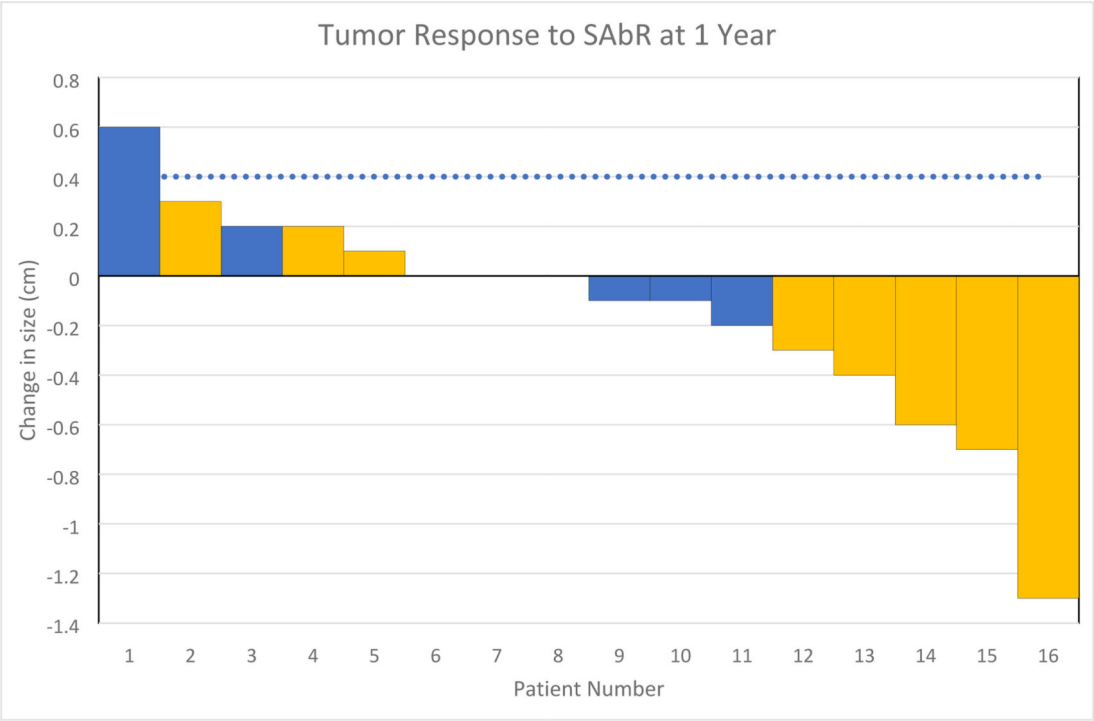

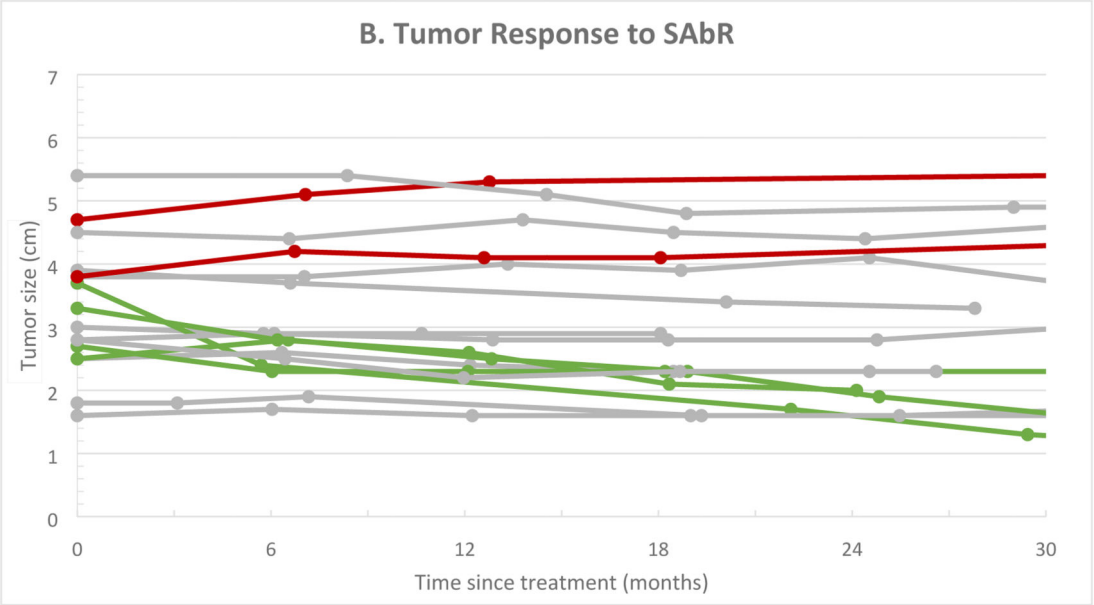

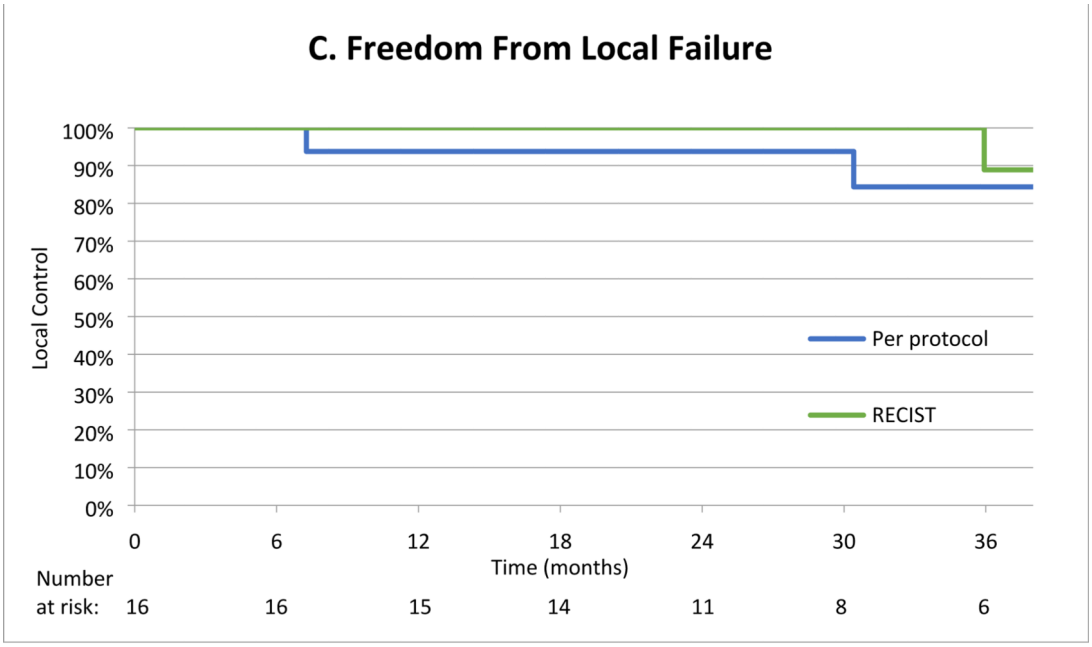

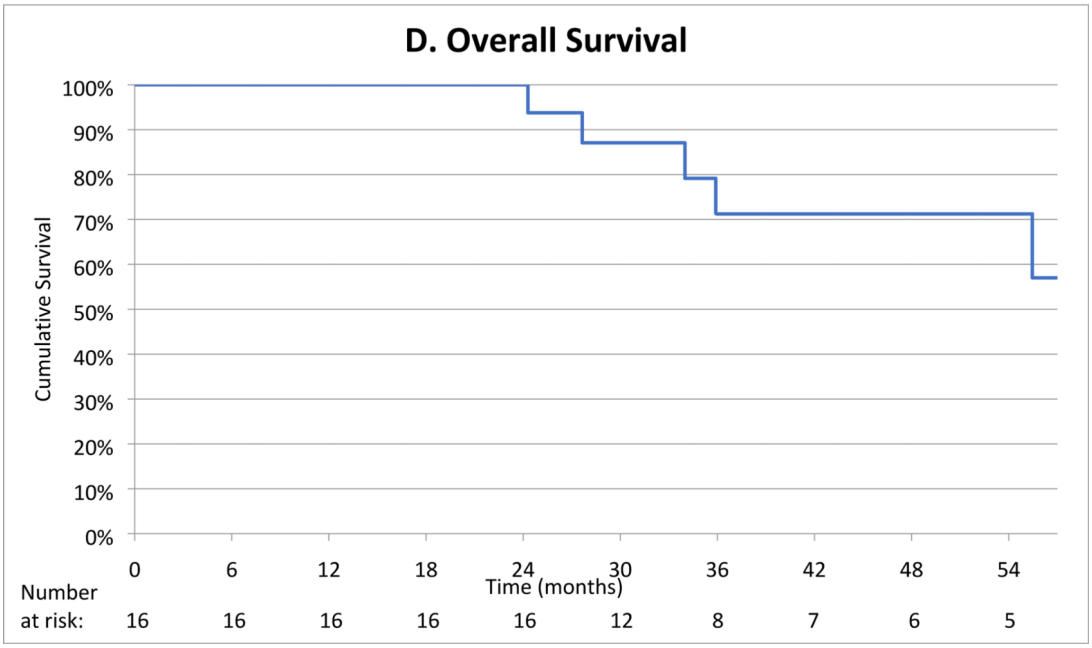

Fig. 2 –.

Tumor response and overall survival. (A) Tumor response to SAbR at 1 year. Blue bars represent patients treated with 40 Gy in five fractions, while gold bars represent patients treated with 36 Gy in three fractions. (B) Patient tumor growth kinetics over time. Failure by per-protocol criteria is shown in red ($n = 2$), while partial responses by RECIST are shown in green ($n = 3$). (C) LC over time per protocol (blue line) and by RECIST criteria (green line). One patient failed by protocol analysis at 6 mo and by RECIST criteria at 36 mo, while another failed by protocol alone after 18 mo. (D) Overall survival is shown, with five

patients dying of noncancer causes during the follow-up period. LC = local control; RECIST = Response Evaluation Criteria in Solid Tumors; SAbR = stereotactic ablative radiotherapy.

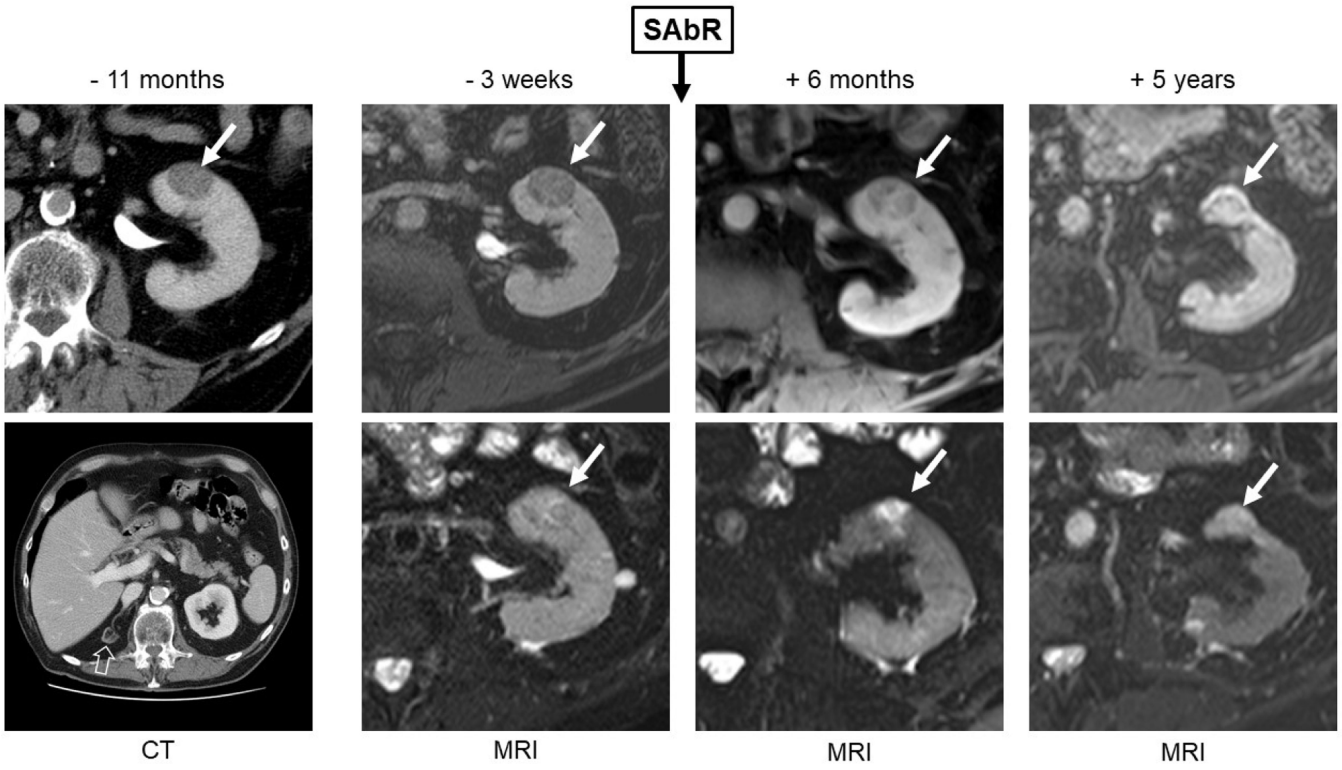

Fig. 3 –.

Initial computed tomography (CT) obtained 11 mo prior to SAbR, magnetic resonance imaging (MRI) obtained 3 wk prior to SAbR, and surveillance MRI at 6 mo and 5 yr after SAbR of a patient with a single functional kidney (ie, congenital atrophic right kidney; open arrow on baseline CT) and a left renal mass (solid arrow). Percutaneous biopsy confirmed grade 3 clear cell renal cell carcinoma. The renal mass exhibited growth from 2.5 cm (11 mo prior to SAbR) to 2.7 cm (baseline, 3 wk prior to SAbR). The patient was treated with 36 Gy in five fractions. Follow-up MRI showed a decrease in size on initial follow-up to 2.3 cm (6 mo after SAbR) and subsequently to 1.9 cm (5 yr after SAbR). T1-weighted fat-saturated gradient-echo contrast-enhanced images obtained during the delayed nephrographic phase (top row) show progressively increased enhancement after SAbR, while T2-weighted images (bottom row) show increased signal intensity after treatment suggestive of treatment-induced fibrosis in the renal mass. SAbR = stereotactic ablative radiotherapy.

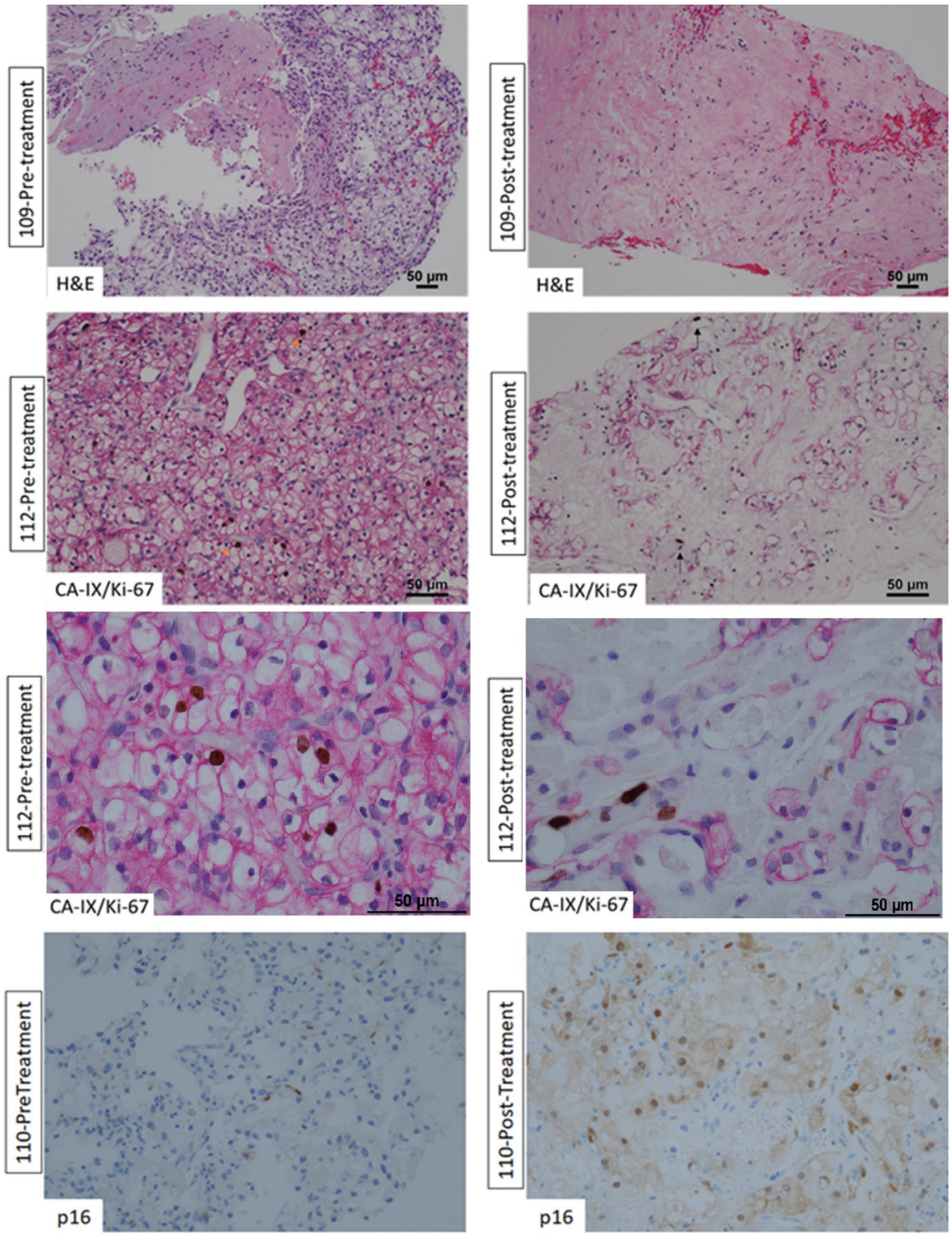

Fig. 4 –.

Representative pre- and post-treatment histologic images for three patients. (A) Pretreatment staining for patient 109 shows tumor cells with minimal hyalinization. (B) After treatment, the same patient had significant hyalinization (99%, top right) and reduction in the number of tumor cells. Similarly, (C and D) tumor tissue taken from patient 112 (lower and higher magnification panels) shows Ki-67 (brown nuclear staining) in tumor cells (E) stained with membranous CAIX (magenta stain; orange arrow). (F) Post-treatment tissue from the same patient shows significant reduction in the number of tumor cells with Ki-67 expression

limited to endothelial cells (black arrow). For patient 110, (G) the post-treatment staining shows significant p16 expression (bottom right) by tumor cells as compared with (H) pretreatment staining (bottom left) where p16 is not seen. H&E = hematoxylin and eosin.

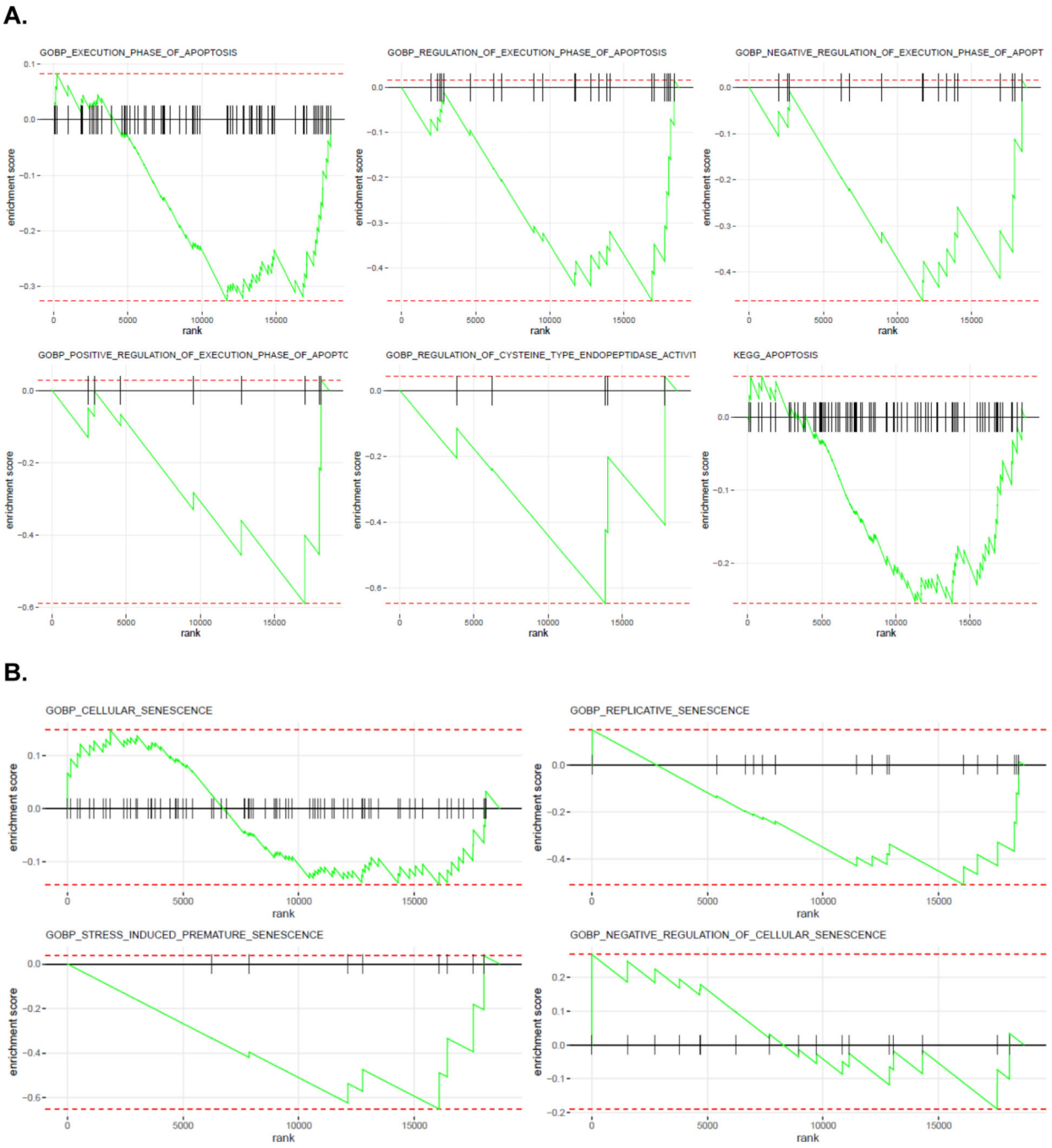

Fig. 5 –.

GSEA of whole transcriptomic data for enriched tumor cells using NanoString GeoMx DSP comparing pre- and post-SAbR treatment biopsy samples focusing on (A) apoptosis and (B) senescence. GSEA = gene set enrichment analysis; SAbR = stereotactic ablative radiotherapy.

Table 1 –

Baseline demographic characteristics (n = 16)

Characteristic (range)	Category	Value
Age (yr)	Median (IQR)	72 (65–80)
Sex, n (%)	Male	11 (69)
Laterality, n (%)	Right	10 (63)
Initial size (cm)	Median (IQR)	3.2 (2.6–3.9)
Baseline growth rate (cm/yr)	Median (IQR)	0.8 (0.3–1.4)
T1 substage (AJCC 8th edition), n (%)	T1a	13 (81)
Location, n (%)	Exophytic	8 (50)
Treatment fractionation, n (%)	36 Gy in 3 fractions	10 (63)
Race/ethnicity, n (%)	White	9 (56)
	Black	6 (38)
	Hispanic	1 (6)
CKD stage, n (%)	1	2 (13)
	2	6 (38)
	3	8 (50)
	4–5	0 (0)
Histology, n (%)	Clear cell	11 (69)
	Papillary	3 (19)
	Other	2 (13)
RENAL score, n (%)	4–6	8
	7–9	8
	10–12	0

AJCC = American Joint Committee on Cancer; CKD = chronic kidney disease; IQR = interquartile range; RENAL = Radius, Exophytic/endophytic, Nearness to the collecting system, Anterior/posterior, Location relative to the polar line [29].

Table 2 –

Pathology data

Patient number	Dose fractionation	Before treatment				After treatment		
		Histology	Necrosis (%)	Hyalinization (%)	Ki-67 (%)	Necrosis (%)	Hyalinization (%)	Ki-67 (%)
101	40 Gy/5 fx	Clear cell	0	5	2	0	20	0
102	40 Gy/5 fx	Clear cell	0	0	5–7	0	*a*	0
103	36 Gy/3 fx		ND	ND	ND	ND	ND	ND
104	36 Gy/3 fx	Clear cell	0	0	4	0	5	1
105	36 Gy/3 fx	Papillary	0	0	2	0	70	1
106	40 Gy/5 fx	Clear cell	NA	NA	NA	2	60	1
107	40 Gy/5 fx	Clear cell	0	0	NA	0	70	1
108	40 Gy/5 fx	Clear cell	20	0	15	2	99	1
109	36 Gy/3 fx	Clear cell	0	0	5–7	0	99	0
110	36 Gy/3 fx	Clear cell	0	5	<1	2	20	<1
111	36 Gy/3 fx	Oncocytic	0	5	1	ND	ND	ND
112	36 Gy/3 fx	Clear cell	0	0	4	2	70	<1
113	40 Gy/5 fx	Clear cell	0	25	<1	0	100	NA
114	36 Gy/3 fx	Papillary	0	0	5–7	NA	NA	NA
115	36 Gy/3 fx	Papillary	0	0	10	95	0	1
116	36 Gy/3 fx	Clear cell	0	5	1–2	ND	ND	ND

Clear cell = clear cell RCC; fx = fractions; NA = no tumor present in tissue evaluated; ND = tissue not available; Oncocytic = oncotic renal tumor, not further classified; Papillary = papillary RCC; RCC = renal cell carcinoma.

*a*Too scant to accurately quantitate.

Table 3 –

Adverse event data

Adverse event [a]	Acute [b]	Late [c]	Overall
Nausea	3	0	3
Vomiting	2	0	2
Creatinine increase	0	2	2
Urinary frequency	1	0	1
Thrombocytopenia	0	1	1
Hematuria	1	0	1
Fatigue	0	1	1
Total	7	4	11

[a] All events were grade 1.

[b] Present in the first 3 mo of follow-up.

[c] Present at longer than 3-mo follow-up.

Table 4 –

Digital spatial protein (GeoMx DSP, NanoString) expression changes

Protein	Mean change from Baseline to 1 yr (*n* = 4 pts/32 samples)	*p* value	False discovery rate adjusted *p* value
Cell death panel			
BAD	−9.87 (−22.8, 3.00)	0.093	0.2
p53	1.50 (−0.56, 3.55)	0.10	0.2
Cleaved Caspase 9	−2.91 (−7.13, 1.31)	0.12	0.2
GZMA	0.09 (−0.07, 0.25)	0.16	0.3
BCLXL	1.28 (−1.00, 3.55)	0.17	0.3
BCL6	0.12 (−0.25, 0.50)	0.4	0.5
BIM	−0.07 (−0.49, 0.34)	0.6	0.7
CD95/Fas	0.14 (−1.10, 1.37)	0.7	0.8
PARP	0.05 (−0.39, 0.50)	0.7	0.8
PI3K/AKT signaling panel			
Pan-AKT	−3.39 (−5.61, −1.16)	0.017	0.14
Phospho-Tuberin (T1462)	0.22 (−0.04, 0.49)	0.077	0.2
PLCG1	−0.15 (−0.43, 0.14)	0.2	0.3
MET	−0.49 (−1.80, 0.81)	0.3	0.5
INPP4B	−0.04 (−0.16, 0.09)	0.4	0.5
Phospho-AKT (Ph T308)	0.05 (−0.08, 0.17)	0.3	0.5
Phospho-PRAS40 (T246)	−1.14 (−4.39, 2.11)	0.3	0.5
Phospho-GSK3B (S9)	−0.05 (−0.21, 0.12)	0.4	0.5
Phospho-GSK3A (S21)/phospho-GSK3B (S9)	0.05 (−0.18, 0.29)	0.5	0.6
MAPK signaling panel			
pan-RAS	0.35 (0.20, 0.49)	0.005	0.13
EGFR	10.2 (3.09, 17.3)	0.020	0.14
Phospho-p38 MAPK (T180/Y182)	0.10 (0.02, 0.17)	0.026	0.14
Phospho-p90 RSK (T359/S363)	2.51 (0.48, 4.54)	0.029	0.14
Phospho-JNK (T183/Y185)	0.11 (0.02, 0.20)	0.030	0.14
Phospho-MEK1 (S217/S221)	0.09 (0.00, 0.18)	0.046	0.17
BRAF	0.43 (−0.00, 0.85)	0.051	0.17
Phospho-p44/42 MAPK ERK1/2 (T202/Y204)	4.99 (−0.92, 10.9)	0.075	0.2
p44/42 MAPK ERK1/2	0.11 (−1.43, 1.66)	0.8	0.8

CI = confidence interval; MAPK = mitogen-activated protein kinase; PI3K = phosphoinositide 3-kinase; pts = patients.

Baseline and 1-yr post-treatment data showing mean protein expression (95% CI).